

SENSITIVITY ANALYSIS OF MULTIPLE FAULT TEST AND RELIABILITY MEASURES IN INTEGRATED GPS/INS SYSTEMS

Ali Almagbile¹, Jinling Wang², Weidong Ding³, Nathan. Knight⁴

^{1,2,3,4} School of Surveying and Spatial Information Systems - University of New South
Wales- Sydney – NSW 2052-Australia

¹ a.almagbile@student.unsw.edu.au, ² jinlin.wang@unsw.edu.au,

³ weidong.ding@unsw.edu.au, ⁴ n.knight@student.unsw.edu.au

KEY WORDS: GPS/INS integration, Kalman filtering, Multiple faults, Reliability measures, Sensitivity analysis,

ABSTRACT: Based on Kalman filtering, multi-sensor navigation systems, such as the integrated GPS/INS system, are widely accepted to enhance the navigation solution for various applications. However, such integrated systems do not always provide robust and stable navigation solutions due to unmodelled measurements and system dynamic errors, such as faults that degrade the performance of Kalman filtering for such integration. Single fault detection methods based on least squares (snapshot) method were investigated extensively in the literature and found effective to detect the fault at either sensor level or integration level. However, the system might be contaminated by multiple faults simultaneously. Thus, there is an increased likelihood that some of the faults may not be detected and identified correctly. This will degrade the accuracy of positioning. In this paper multiple fault test and reliability measures based on a snapshot method were implemented in both the measurement model and the predicted states model for use in a GPS/INS integration system. The influences of the correlation coefficients between fault test statistics on the performances of the faults test and reliability measures were also investigated. The results indicate that the multiple fault test and reliability measures can perform more strength effectively in the measurement model than the predicted states model due to weak geometric strength within the predicted states model.

1. INTRODUCTION

Today integrated navigation systems have been widely employed to provide robust and reliable navigation solutions for various platforms such as land-based vehicles or unmanned aerial vehicles (UAVs). The Kalman filtering has been commonly used as a data fusion tool for the integration of GPS/INS in real-time kinematic applications. In all GPS/INS application scenarios, quality control technique should be implemented in either system level or integration level in order to minimize the unpredicted failures (outliers/faults) which are considered as biases in functional models. Faults can be considered as the measurements that deviate considerably from the normal distribution for the majority of the measurements within the systems. The appearance of the faults in the systems may degrade the navigation solution at any stage of navigation. Therefore, quality control technique including integrity and the reliability of the navigation solutions is employed to provide an alert to the user when the system is no longer available for reliable navigation. The reliability deals with minimizing the failures whereas the integrity is to detect if the fault has occurred and then isolate/remove it in order to achieve high reliability of the system.

With high degree of the integrity, the reliability of the system will increase (Sukkarieh, 2000).

In order to check the influence of the faults on the observations, the reliability theory was introduced by Baarda (1968) and applied to the geodetic survey to evaluate the ability of a system to control measurements. The reliability theory includes internal reliability, such as Minimal Detectable Bias (MDB) which is also known as Marginally Detectable Error (MDE), controllability and reliability numbers to evaluate the ability of the model to detect the faults. The reliability number is used to remove the effect of non-centrality parameter. The internal reliability of the system is influenced by some factors such as the correlated and non-correlated observations, the number of visible satellites, geometric constrains, multi-sensor integration system and the structure of dynamic model.

Förstner (1983) extended the reliability theory through evaluating the alternative hypothesis. Furthermore, the theory has been assessed in the cases of correlated and uncorrelated observations. With correlated observations, Wang and Chen (1994) proposed a new reliability measures for single fault and found that the range of the redundancy number may exceed one or become negative, when the observations are correlated. Similarly, Proszynski (2010) introduced another approach to reliability measures with correlated observations. In multi-sensor integration systems, Hewitson and Wang (2010) implemented the reliability theory under single fault scenario in GNSS/INS integration system. Recently, Knight et al (2010) extended the reliability theory by generalizing a new mathematical computation of internal and external reliability under the presence of multiple faults.

In this paper, multiple fault test and reliability measures in terms of Minimal Detectable Bias (MDB) and reliability number have been implemented for tight GPS/INS integration systems. Fault detection tests and reliability measures have been applied under the scenarios of single and multiple faults in measurement and predicted state models. In order to evaluate the performances of the fault detection test, the correlation coefficients between the fault detection tests statistics have been analysed for measurements and predicted states models.

The structure of the paper is as follows: Section 2, describes the mathematical model of multiple faults and reliability measures in GPS/INS systems. Section 3, provides the test and the results followed by the concluding remarks in section 4.

2. MULTIPLE FAULTS IN GPS/INS SYSTEMS

Kalman filtering is normally employed for tight GPS/INS integration and the discrete time of the system state and measurement model of the Kalman filtering can be written as follows:

$$x_k = \Phi_{k-1}x_{k-1} + w_{k-1} \quad (1)$$

$$z_k = H_k x_k + v_k \quad (2)$$

where x_k is the $(n \times 1)$ state vector; Φ_k is the $(n \times n)$ transition matrix; z_k is the $(r \times 1)$ observation vector; H_k is the $(r \times n)$ observation matrix. The variables w_k and v_k are uncorrelated white noise errors with covariance matrices Q_k and R_k respectively.

It has been found that through integrating the predicted states \bar{x}_k and the measurement model z_k of Kalman filtering in one vector using least squares principles, optimal estimate of the state parameters can be obtained. The corresponding measurement model can be expressed as (Wang et al, 2008):

$$l_k = A_k x_k + v_k \quad (3)$$

$$l_k = \begin{bmatrix} z_k \\ \bar{x}_k \end{bmatrix}, A_k = \begin{bmatrix} H_k \\ E \end{bmatrix}, v_k = \begin{bmatrix} v_{zk} \\ v_{\bar{x}k} \end{bmatrix} \quad (4)$$

where E is the $m_k \times m_k$ identity matrix

The corresponding variance- covariance matrix, which is derived from the measurement noise covariance matrix R and the predicted states covariance matrix $P(-)$ of Kalman filtering, can be written as (Wang et al, 2008) :

$$C_{l_k} = \begin{bmatrix} R_k & 0 \\ 0 & \bar{P}_k \end{bmatrix} \quad (5)$$

The optimal estimate of the state parameters \hat{x}_k and the error covariance matrix $Q_{\bar{x}k}$ are:

$$\hat{x}_k = (A_k^T C_{l_k}^{-1} A_k)^{-1} A_k^T C_{l_k}^{-1} l_k \quad (6)$$

$$Q_{\bar{x}k} = (A_k^T C_{l_k}^{-1} A_k)^{-1} \quad (7)$$

The KF residuals v_k and cofactor Q_{v_k} can then be calculated from:

$$v_k = \begin{bmatrix} v_{zk} \\ v_{\bar{x}k} \end{bmatrix} = A_k x_k - l_k \quad (8)$$

$$Q_{v_k} = C_{l_k} - A_k Q_{\bar{x}k} A_k^T \quad (9)$$

The Kalman filtering as least squares (snapshot) can be used for fault detection test in integrated GPS/INS systems.

2.1. Faults detection test

After employing the global model test to test whether the model includes faults or not, the fault detection test can be used in order to identify the corresponding measurements as

a fault. Regardless the true number of faults that exist in the observations, the fault detection test can be written as follows (Wang and Chen, 1999; Knight et al, 2010):

$$w^2 = \frac{l^T C_l^{-1} Q_v C_l^{-1} G (G^T C_l^{-1} Q_v C_l^{-1} G)^{-1} G^T C_l^{-1} Q_v C_l^{-1} l}{\sigma_0^2} \sim \chi_{1-\alpha, \theta}^2 \quad (10)$$

Where G is an n by θ matrix, with rank θ containing zeros with a one in each column corresponding to the fault, σ_0^2 is the priori variance . When w^2 exceeds the predefined critical value, the null hypothesis will be rejected because one or more faults exist in the observations. Since the alternative hypothesis is accepted, the fault detection test statistics will have a non-central Chi-square distribution and then the non-centrality parameter can be written as (Baarda, 1968; Wang and Chen, 1999):

$$\lambda = \frac{z^T G^T C_l^{-1} Q_v C_l^{-1} G z}{\sigma_0^2} \quad (11)$$

where z is the true fault vector, if the fault identification is possible, the largest w^2 test is corresponding to the true fault vector. Faults identification based on (10) can be applied for different number of faults such as one, two or three faults. The procedure is to apply (10) for single fault and remove the fault if it exists, then to two faults, three and so on.

2.2. Internal reliability measures

With given a certain probabilities of Type I error α and Type II errors β , the internal reliability of the system which includes the Minimal Detectable Bias (MDB) $\nabla_0 S_i$ and the reliability numbers r_i can be calculated in order to evaluate the system ability for detecting faults in the model. MDB for single fault can be determined as (Baarda, 1968; Salzmann, 1993; Gikas et al, 1999; Knight et al 2010):

$$\nabla_0 S_i = \sqrt{\frac{\lambda \sigma_0^2}{h_i^T C_l^{-1} Q_v C_l^{-1} h_i}} \quad (12)$$

where h_i is $(1 \times n)$ vector containing zeros and one elsewhere corresponding to the single fault. For multiple faults ($\theta=2$ or more) however, the MDB can be computed through determining the multiple correlation coefficients. In the case of two faults, the multiple correlation is equivalent to the correlation coefficients between two single fault tests statistics. The multiple correlation coefficients P_{ij}^θ and MDB for multiple faults $\nabla_0 S_i^\theta$ can then be written respectively as (Knight et al., 2010):

$$P_{ij}^{\theta} = \sqrt{\frac{h_i^T C_l^{-1} Q_v C_l^{-1} G_j (G_j^T C_l^{-1} Q_v C_l^{-1} G_j)^{-1} G_j^T C_l^{-1} Q_v C_l^{-1} h_i}{h_i^T C_l^{-1} Q_v C_l^{-1} h_i}} \quad (13)$$

With bounds of P_{ij}^{θ} are: $0 \leq P_{ij}^{\theta} \leq 1$

$$\nabla_0 S_i^{\theta} = \sqrt{\frac{\lambda \sigma_0^2}{h_i^T C_l^{-1} Q_v C_l^{-1} h_i (1 - P_{ij}^{\theta})}} \quad (14)$$

in order to evaluate the impact of the system geometry, reliability number can be used. Reliability number can be calculated in the cases of single and multiple faults respectively as (Wang & Chen 1994; Knight et al 2010):

$$r_i = h_i^T C_l h_i h_i^T C_l^{-1} Q_v C_l^{-1} h_i \quad (15)$$

$$r_i^{\theta} = h_i^T C_l h_i h_i^T C_l^{-1} Q_v C_l^{-1} h_i (1 - P_{ij}^{\theta}) \quad (16)$$

It has been proved that when observations are not correlated the reliability number is equal to the redundancy number \bar{r}_i (Wang & Chen 1994):

$$\bar{r}_i = h_i^T Q_v C_l^{-1} h_i = r_i \quad (17)$$

With bounds of $0 \leq r_i \leq 1$ (18)

In the case of correlated observations however, the bounds of r_i for single and multiple faults can be written respectively as:

$$0 \leq r_i \leq h_i^T Q_v C_l^{-1} h_i \quad (19)$$

$$0 \leq r_i^{\theta} \leq h_i^T C_l h_i h_i^T C_l^{-1} Q_v C_l^{-1} h_i (1 - P_{ij}^{\theta}) \quad (20)$$

3. TEST AND RESULTS

Tight GPS/INS integration experiments have been carried out using the real data set calculated by two dual frequency Leica 530 GPS receivers and one **BEI C-MIGITSII (DQI-NP)** INS unit. One of the GPS receivers was static and another one along with **DQI-NP** was set on the top of a land-based vehicle. Figure 1 shows vehicle trajectory of the moving receiver. GPS receivers tracked 8 satellites at the first 20 epochs and then the number of satellites fluctuated around 6 until they ended up with 7 satellites.

Pesudo-range observations for tight GPS/INS integration were used to update 15 error states: 9 states of navigation solution (3 for the position errors, 3 for the velocity errors and 3 for the attitude errors), 3 states for the INS acceleration biases, and the last 3 for the gyro biases.

In order to evaluate the performance of the fault detection test statistics in integrated GPS/INS systems, faults were injected (simulated) in measurement and predicted states models at different locations. The fault detection test as well as reliability measures were applied to detect and identify single and multiple faults, as well as to measure the fault detection ability, in measurement and predicted states models.

3.1. Fault tests and internal reliability in measurement model

Fault detection test statistics and internal reliability measures for single fault scenario in measurements model at epoch 10 are shown in Table 1. When 12m fault was added to satellite 18, the fault test identifies that satellite as a faulty satellite because the value of the fault detection test exceeds the critical value (CV) which is 10.83 with alpha (α) and beta (β) equal to 0.1% and 80% respectively. The Minimal Detectable Bias (MDB) for the faulty satellite is less than simulated fault value, indicating the ability of the test to identify the fault. When satellite 18 was removed, the values of of fault detection test statistic increased slightly but it was less than the critical value.

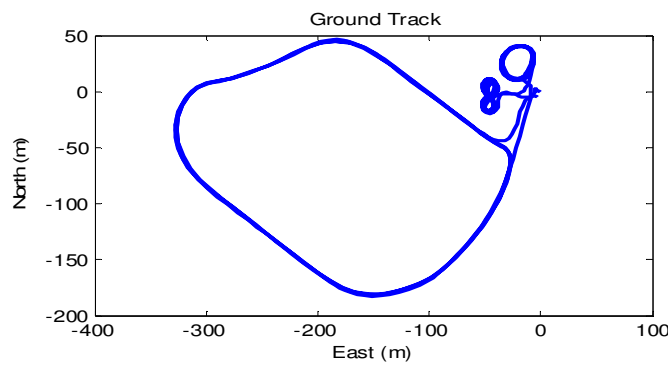


Fig. 1. Vehicle trajectory

In order to show the behaviour of MDB and reliability number with time, Figure 2 shows the averaged MDB and reliability number, as well as the number of visible satellites over the time. It is obvious that opposite relationships can be seen when comparing these three graphs in Figure 2. When the number of visible satellites increases, the reliability number increases as well. Normally, when the number of visible satellites increases, the MDB decreases and vice versa.

Regarding the two faults scenario, Table 2 shows the faults of 12m at measurements 5 and 6. The critical value is 13.82 (with the alpha being equal to 0.1%). In a normal situation, the value of the fault detection test statistics for all the measurement pairs related to measurements 5 or 6 should exceed the critical value. It is obvious that, the value of the fault test statistic for both (5,6) measurements is the highest value that exceeds the critical value. However, other values for the measurement pairs such as (1,3), (1,4) and (3,4) measurements failed the test too, because they are higher than the critical value. The most likely reason is related to the correlation coefficients between the fault test statistics. More

analysis about correlation coefficients between fault test statistics will be highlighted later in this paper.

The internal reliability for the multiple fault test scenario is shown in Table 3. Due to the limited space herein, only MDB and reliability number for 5 and 6 measurements are shown. It can clearly be seen that the MDB is smaller than the simulated fault values. Therefore, the fault test for identifying measurements 5 and 6 as faulty measurements is efficient.

Tab. 1. Single fault test statistics and internal reliability at epoch 10 in GPS/INS integration ($\alpha=0.1\%$, $\beta=80\%$, $CV=10.83$)

| One Fault of 12m in measurement 5 (SV 18) | | | | SV 18 Removed | | |
|---|--------------|--------------|--------------|---------------|-------------|-------|
| SV | Wi^2 | MDB_i (m) | ri | Wi^2 | MDB_i (m) | ri |
| 3 | 0.057 | 4.758 | 1.696 | 1.231 | 4.794 | 1.671 |
| 6 | 0.093 | 6.050 | 1.049 | 0.582 | 6.071 | 1.040 |
| 14 | 2.057 | 5.252 | 1.392 | 2.109 | 5.168 | 1.442 |
| 15 | 2.925 | 5.363 | 1.335 | 0.521 | 5.362 | 1.343 |
| 18 | 46.43 | 5.290 | 1.372 | | | |
| 21 | 0.059 | 5.993 | 1.069 | 4.794 | 5.19 | 1.431 |
| 22 | 0.765 | 5.597 | 1.226 | 0.362 | 5.646 | 1.201 |
| 26 | 0.001 | 4.651 | 1.775 | 0.015 | 4.622 | 1.801 |

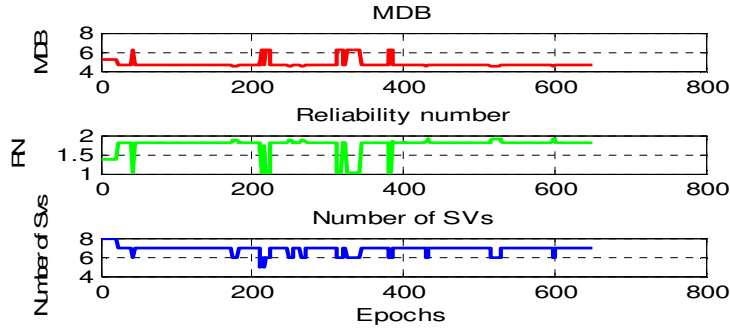


Fig. 2. The averaged MDB/reliability number for single fault test and the number of visible satellites over the time for measurement model

3.2. Fault tests and internal reliability in predicted states model

In this section, a fault of 15m were injected in predicted states in order to be tested using both single and multiple fault detection tests. All conditions in terms of critical value, alpha, and beta are similar to those used in the measurement model. In Table 4, the fault detection test identified a single fault in Y position because its value exceeds the critical value. Furthermore, Y velocity and X attitude are also identified as faults due to the high

correlation coefficients between them and the observation that includes the true fault. The performance of single fault detection test is efficient because the MDB value is smaller than the simulated fault value.

Figure 3 shows the average of MDB, reliability number for predicted states and the number of visible satellites over the time. It is obvious that the opposite relationships can be seen when comparing the three graphs in Figure 3. When the number of visible satellites increases, the reliability number increases as well. And at the same time, however, the opposite relationship between the MDB and the number of visible satellites can be seen.

Tab. 2. Multiple fault test statistics at epoch 10 in GPS/INS integration ($\alpha=0.1\%$, $\beta=80\%$, $CV=13.82$)

| Two faults of 12m in measurements 5 and 6 (SV 18 & 21) | | | | | | | | | | | |
|--|----------|---------------|----------|----------|--------------|----------|----------|---------------|----------|----------|---------|
| <i>i</i> | <i>j</i> | W_i^2 | <i>i</i> | <i>j</i> | W_i^2 | <i>i</i> | <i>j</i> | W_i^2 | <i>i</i> | <i>j</i> | W_i^2 |
| 1 | 2 | 13.318 | 2 | 5 | 25.926 | 4 | 5 | 48.812 | | | |
| 1 | 3 | 35.549 | 2 | 6 | 35.977 | 4 | 6 | 46.813 | | | |
| 1 | 4 | 24.139 | 2 | 7 | 2.411 | 4 | 7 | 13.242 | | | |
| 1 | 5 | 42.146 | 2 | 8 | 3.079 | 4 | 8 | 13.067 | | | |
| 1 | 6 | 54.926 | 3 | 4 | 21.58 | 5 | 6 | 59.375 | | | |
| 1 | 7 | 16.131 | 3 | 5 | 47.423 | 5 | 7 | 25.682 | | | |
| 1 | 8 | 16.039 | 3 | 6 | 46.424 | 5 | 8 | 26.385 | | | |
| 2 | 3 | 15.708 | 3 | 7 | 15.275 | 6 | 7 | 35.328 | | | |
| 2 | 4 | 13.518 | 3 | 8 | 15.519 | 6 | 8 | 38.236 | | | |
| | | | | | | 7 | 8 | 3.331 | | | |

Tab. 3. Internal reliability for two faults in the measurement model at epoch 10 ($\alpha=0.1\%$, $\beta=80\%$, $CV=13.82$, $\theta=2$)

| <i>i</i> | <i>j</i> | MDB_i (m) | r_i | <i>i</i> | <i>j</i> | MDB_i (m) | r_i |
|----------|----------|----------------|-------|----------|----------|----------------|-------|
| 5 | 1 | 5.304 | 1.372 | 6 | 1 | 6.035 | 1.059 |
| 5 | 2 | 5.309 | 1.360 | 6 | 2 | 5.998 | 1.151 |
| 5 | 3 | 5.372 | 1.352 | 6 | 3 | 6.006 | 1.048 |
| 5 | 4 | 5.479 | 1.348 | 6 | 4 | 5.993 | 1.089 |
| 5 | 6 | 5.291 | 1.375 | 6 | 5 | 5.994 | 1.069 |
| 5 | 7 | 5.314 | 1.355 | 6 | 7 | 6.020 | 1.068 |
| 5 | 8 | 5.293 | 1.376 | 6 | 8 | 6.021 | 1.067 |

Table 5 shows multiple fault test for two faults in predicted states 2 and 7 (observation 10 and 15 respectively) and also internal reliability of observation 10 only. When the faults were added in observations 10 and 15, the fault detection test identified those observations as faulty. Similar to the measurement model case, the value of the fault detection test statistics for all the observations that related to the 10 or 15 should exceed the critical value. It is obvious that, the value of the fault test statistic for both (10,15) is the highest value among all the observations. It can also be seen that observations (10,13) and (13,15) have very high values. This is due to the correlation coefficients between the fault detection test statistics. One can see that the MDB values increase, while the reliability number values decrease.

3.3. Correlation coefficients analysis

The correlation coefficients between two fault detection test statistics w_i and w_j are an efficient indicator of the performance of the fault test statistics. When the correlation coefficients between the tests statistics are high, the identification of the faults becomes difficult and hence several observations may be flagged as faulty observations wrongly. Since Kalman filter as least squares is used in integrated GPS/INS system, the characteristics of the observation vector components are varied due to the heterogeneity of the observations, which then leads to complex correlation coefficients between the tests statistics and consequently, more difficulties in identifying the correct faults, especially in the predicted states model.

Tab. 4 Single fault test statistics and internal reliability at epoch 10 in GPS/INS integration ($\alpha=0.1\%$, $\beta=80\%$, $CV=10.83$)

| Fault of 15m in observation 10 (predicted state 2) | | | | |
|--|-----------|---------------|---------------|--------------|
| State | Obs | W_i^2 | MDB_i | r_i |
| Position | 9 | 2.632 | 4.651 | 10.174 |
| | 10 | 20.185 | 7.719 | 6.215 |
| | 11 | 3.803 | 7.580 | 6.691 |
| velocity | 12 | 0.733 | 9.329 | 4.237 |
| | 13 | 14.072 | 10.042 | 3.314 |
| | 14 | 0.413 | 9.950 | 4.161 |
| Attitude | 15 | 12.778 | 10.884 | 2.854 |
| | 16 | 0.008 | 0.988 | 12.861 |
| | 17 | 0.0172 | 0.988 | 12.861 |
| Acceleration bias | 18 | 0.417 | 1.753 | 13.017 |
| | 19 | 0.052 | 1.298 | 13.217 |
| | 20 | 0.041 | 1.298 | 13.217 |
| Gyro bias | 21 | 0.001 | 1.279 | 13.420 |
| | 22 | 0.02 | 1.002 | 14.221 |
| | 23 | 0.101 | 1.002 | 14.221 |

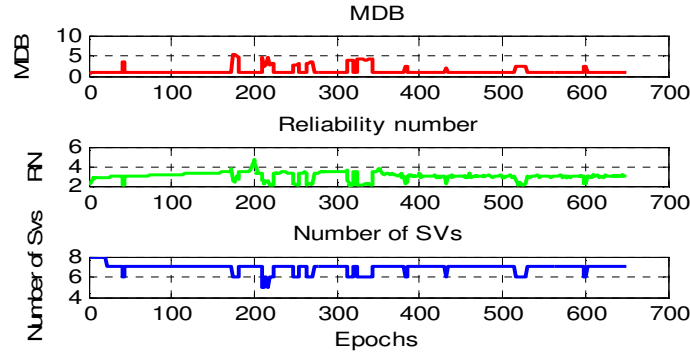


Fig. 3. The averaged MDB/reliability number for single fault test and the number of visible satellites over the time for predicted states in GPS/INS integration

Tab. 5 Multiple fault test statistics and internal reliability for predicted states 2 and 7 (observation 10 and 15 respectively) at epoch 10 in GPS/INS integration ($\alpha=0.1\%$, $\beta=80\%$, $CV=13.82$)

| Two faults of 15 m in predicted states 2 and 7 (observations 10 and 15) | | | | | | | | | |
|---|-----|--------|--------|--------|-----|-----|--------|--|--|
| i | j | Wi^2 | $MDBi$ | ri | i | j | Wi^2 | | |
| 9 | 10 | 31.139 | 0.982 | 10.701 | 9 | 15 | 35.096 | | |
| 11 | 10 | 31.139 | 0.981 | 11.283 | 10 | 15 | 70.752 | | |
| 12 | 10 | 31.139 | 0.986 | 13.423 | 11 | 15 | 35.128 | | |
| 13 | 10 | 59.124 | 11.917 | 1.771 | 12 | 15 | 35.085 | | |
| 14 | 10 | 31.139 | 0.981 | 11.283 | 13 | 15 | 61.704 | | |
| 15 | 10 | 70.752 | 8.107 | 1.908 | 14 | 15 | 35.095 | | |
| 16 | 10 | 31.139 | 0.993 | 10.628 | 16 | 15 | 35.077 | | |
| 17 | 10 | 31.14 | 1.309 | 10.201 | 17 | 15 | 35.077 | | |
| 18 | 10 | 31.431 | 1.649 | 9.906 | 18 | 15 | 35.077 | | |
| 19 | 10 | 31.169 | 0.965 | 10.718 | 19 | 15 | 35.077 | | |
| 20 | 10 | 31.139 | 0.974 | 9.651 | 20 | 15 | 35.873 | | |
| 21 | 10 | 31.139 | 0.990 | 10.001 | 21 | 15 | 35.077 | | |
| 22 | 10 | 31.139 | 0.985 | 11.719 | 22 | 15 | 35.077 | | |
| 23 | 10 | 31.139 | 0.983 | 10.991 | 23 | 15 | 35.077 | | |

Figure 4 shows the correlation coefficients between the fault detection test statistics for the measurement model, the predicted state model and measurement with predicted states. One can see that the correlation coefficients matrix is symmetric with diagonal ones showing that each measurement is fully correlated with itself. For the measurement model only, the degree of correlation coefficients is small and the highest degree comes between (4,5) then (3,5) and (3,4). Therefore; if the fault occurs in measurement 5, measurements 3 and 4 may be potentially identified as faulty. This is true based on multiple fault test statistics shown

in Table 2. The worst case can be found in the predicted states model only because they have the highest correlation coefficients. The reason could be related to the functional relationship between the system states model. For instance, the degree of correlation between velocity and position, acceleration bias and gyro bias is very high due to functional relationship (dependency) between them. If the fault occurs in velocity the position will be contaminated as well. Another important point is that the range between the maximum and the minimum values of the correlation coefficients is very high. This is due to the heterogeneous characteristics of the predicted states.

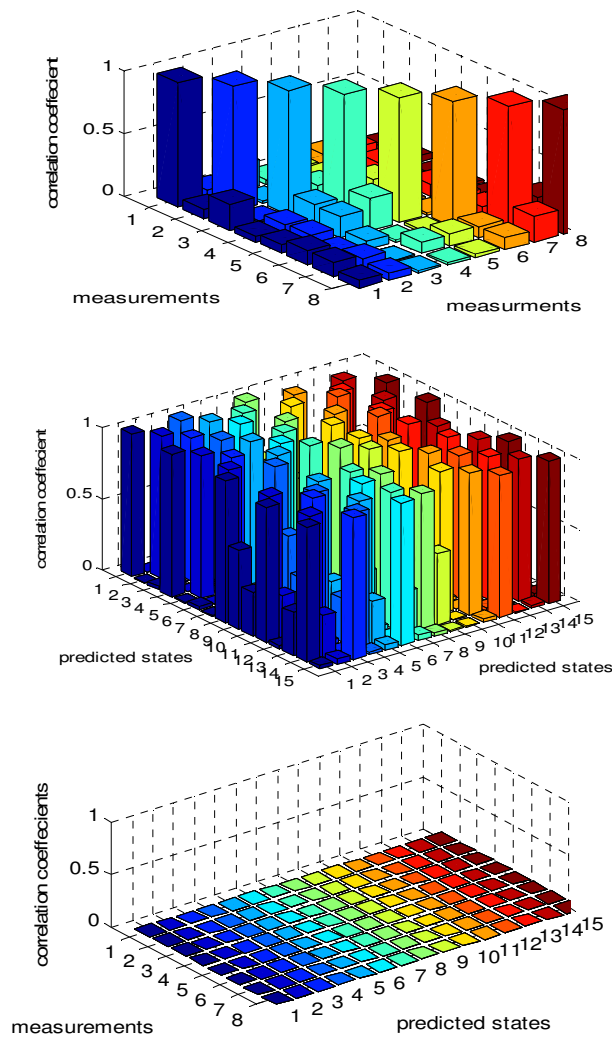


Fig. 4. The correlation coefficients between fault test statistics for the measurement model (top), the predicted state model (middle) and measurements/predicted state models (bottom) at epoch 10 in GPS/INS integration

Between the measurement and predicted states models, the degree of correlation is close to zero. This confirms that there is no strong geometric relationship between the measurement model and the predicted states model and hence if the fault occurs in the measurement model, it may not affect the predicted states model and vice versa.

4. CONCLUDING REMARKS

Multiple fault detection tests and reliability measures in terms of Minimal Detectable Bias (MDB) and reliability number have been investigated in tight GPS/INS integration systems. The paper has analysed the sensitivity of the fault detection test and reliability measures under the presence of single and two faults in both the measurement and predicted state models.

It has been shown that the fault detection tests can perform effectively in identifying single and multiple faults in both the measurement and predicted state models. and the reliability measures (e.g., MDBs) provides realistic evaluation of the ability of the model to identify the faults. However, there are some factors that influence the performance of fault detection tests and reliability measures such as the number of visible satellites, the strength of geometry and the correlation coefficients between the tests statistics.

As the correlation coefficients is higher for the predicted state model than those for the measurement model, several predicted states may be flagged as faulty observations wrongly. Therefore, more analysis about the influence of the correlation coefficients between fault tests statistics under different dynamic model structures, on the performance of the fault detection test requires further investigation in the future.

REFERENCES

- Baarda, W., 1968. A testing procedure for use in geodetic network, *Netherlands Geodetic Commission, publications on Geodesy, New Series*, Delft, The Netherlands, Vol 2, No 5, pp. 1-97.
- Förstner, W., 1983. Reliability and discernability of extended Gauss-Markov models, *Deutsche Geodätische Kommission (DGK), Report A*, No. 98, pp. 79-103.
- Gikas, V., Cross, P., Ridyard, D., 1999. Reliability analysis in dynamic systems: implications for positioning marine seismic networks, *Geophysics*, 64 (4), pp. 1014-1022.
- Hewitson, S., Wang, J., 2010. Extended receiver autonomous integrity monitoring (eRAIM) for GNSS/INS integration, *Journal of Surveying Engineering*, 136 (1), pp. 13-25.
- Knight, N., Wang, J., Rizos, C., 2010. Generalized measures of reliability for multiple outliers, *J Geod*, 84, pp. 625-635.

Proszynski, W., 2010. Another approach to reliability measures for systems with correlated observations, *J Geod*, 84, pp. 547-556

Salzmann, M., 1993. Least squares filtering and testing for geodetic navigation applications, *Netherlands Geodetic Commission, publications on Geodesy, New Series*, Delft, The Netherlands No. 37, pp. 1-209.

Sukkarieh, S., 2000. Low- Cost, High Integrity, Aided Inertial Navigation Systems for Autonomous Land Vehicles, *PhD Thesis, Department of Mechanical and Mechatronic Engineering*, The University of Sydney, Australia, pp.1-212.

Wang, J., Chen, Y., 1994. On the reliability measure of observations. *Acta Geodaetica et Cartographica Sinica*, English Edition, pp. 42-51

Wang, J., Chen, Y., 1999 Outlier detection and reliability measures for singular adjustment models, *Geomat Res Aust*, 71, pp. 57-72.

Wang, J., Xu, C., Wang, J., 2008 Applications of robust Kalman filtering schemes in GNSS navigation. *Int. Symp. on GPS/GNSS*, Yokohama, Japan, 25-28 November, pp.308-316.